The exceptional X-ray evolution of SN1996cr in High Resolution

Jonathan Quirola
Advisor: Prof. Franz Bauer

Instituto de Astrofísica
Pontificia Universidad Católica de Chile

Pontificia Universidad Católica de Chile

Supernovae

- SNe are stellar explosions that occur as the final stage of stellar evolution.
- SNe are classified in two important groups: thermonuclear and core-collapse.

Why are SNe important?

- Enrich the ISM with heavy elements.
- Contribute to the production of new generation of stellar systems, planets and, maybe, life.
- Through shock-CSM interaction we can infer the structure of the circumstellar medium (CSM), which is strongly related with the stages previous to the SNe explosion.

Supernovae type IIn

- Show narrow emission lines of H and He in their optical spectra thought to arise from a very dense, photoionized CSM produced by the mass-loss of the progenitor star.
- As the X-ray luminosity is proportional to the emission measure, X-ray observatories are particularly sensitive to SNe interacting with relatively dense progenitor CSMs (type IIn).

$$L_X = 4\pi \int \Lambda_{ff}(T_{e,i})\, n_{e,i}^2\, r_i^2\, dr,$$

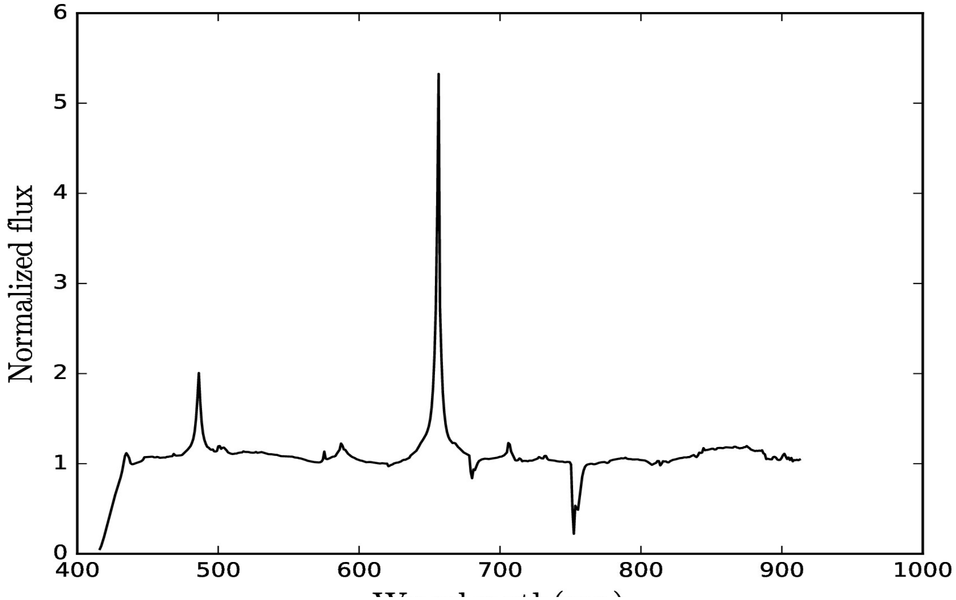

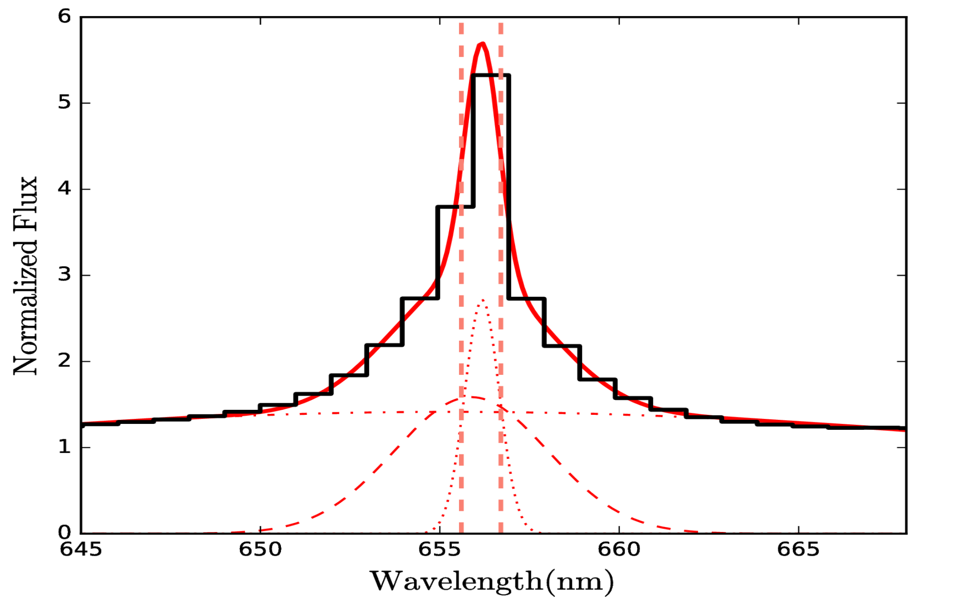

- While more than ~400 SNe IIn are known, only 12 are known to emit in the X-ray bands.
- Most X-ray detected SNe are detected early after explosion and decline with time, but a handful show interactions peaking only after many years. These imply relatively rapid change in the progenitor wind or even eruptive outburst.

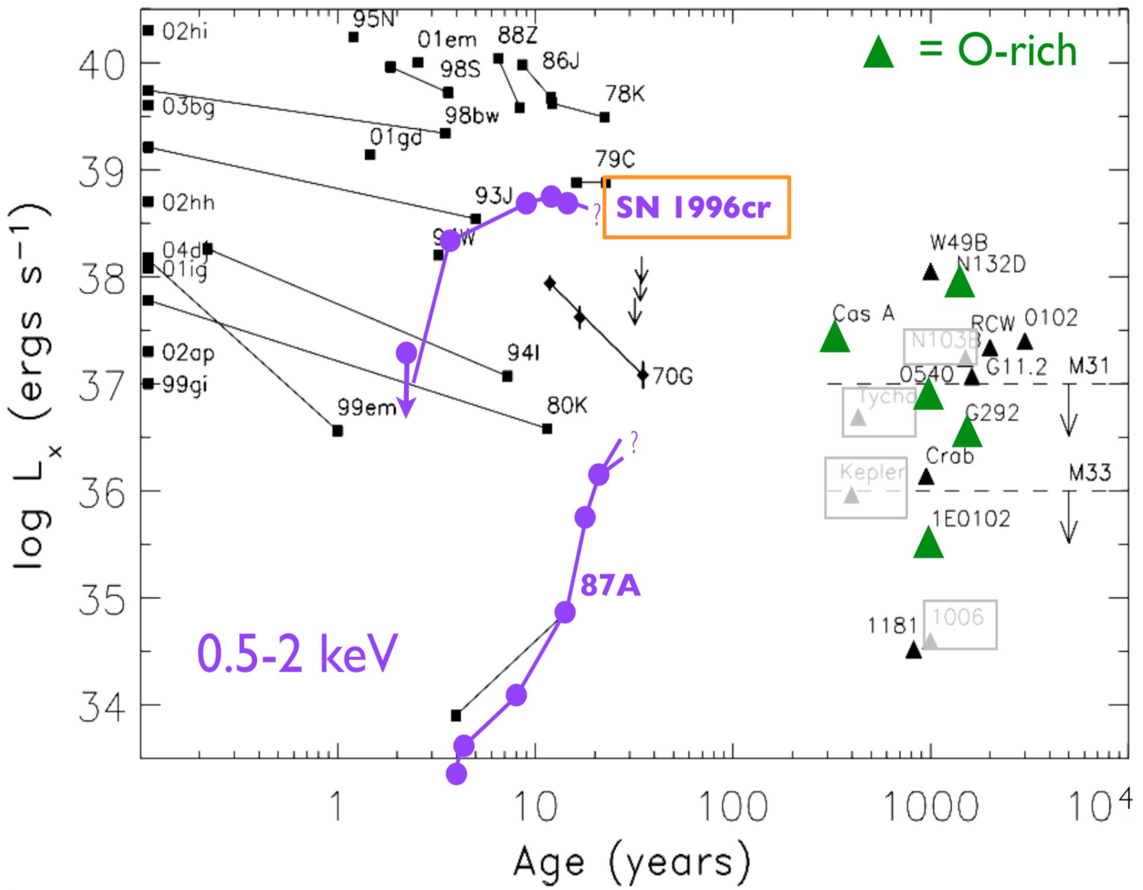

SN1996cr: a case study of an amazing archival object

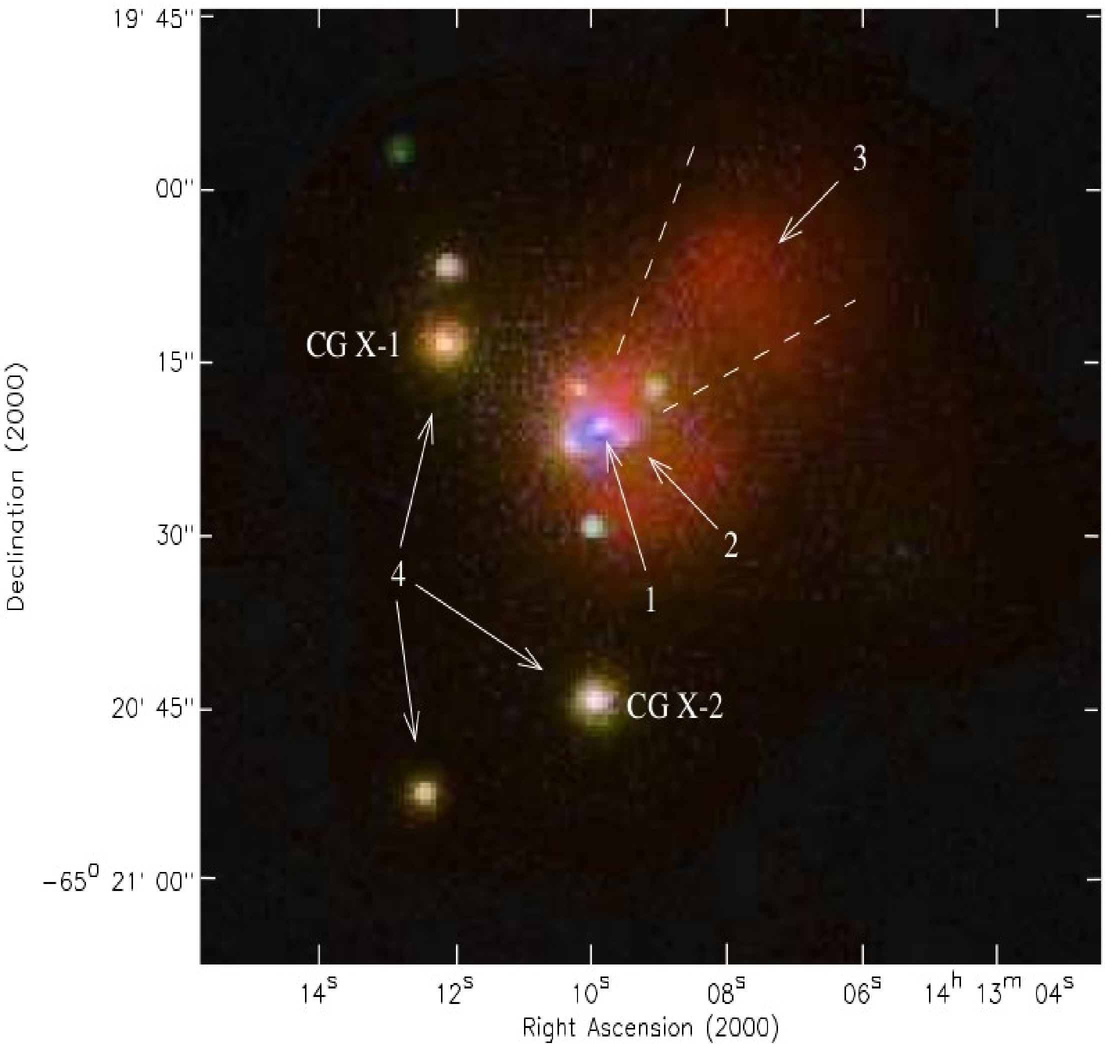

- SN 1996cr was discovered by Chandra as a serendipitous ultraluminous X-ray source (ULXs) in Circinus Galaxy.
- SN 1996cr exploded between 1995-02-28 and 1996-03-16.
- Missed by SNe searches at the time.

Bauer+, 2001

- Several observations in 2000, 2001, 2004 were used to leverage 485 ks in 2009 to study SN1996cr in detail. Later serendipitous XMM data were obtained to follow-up ULXs.

ObsID	Date (UT)	Exposure (ks)	Instruments
374	2000-06-15	7.1	*Chandra* HETG
62877	2000-06-16	60.2	*Chandra* HETG
0111240101	2001-08-06	85.5/91.8/59.5	*XMM-Newton* MOS1/MOS2/*pn*
4770	2004-06-02	55.0	*Chandra* HETG
4771	2004-11-28	59.5	*Chandra* HETG
10223	2008-12-15	102.9	*Chandra* HETG
10224	2008-12-23	77.1	*Chandra* HETG
10225	2008-12-26	67.9	*Chandra* HETG
10226	2008-12-08	19.7	*Chandra* HETG
10832	2008-12-18	20.6	*Chandra* HETG
10833	2008-12-22	28.4	*Chandra* HETG
10842	2008-12-27	36.7	*Chandra* HETG
10843	2008-12-29	57.0	*Chandra* HETG
10844	2008-12-24	27.2	*Chandra* HETG
10850	2009-03-03	16.5	*Chandra* HETG
10872	2009-03-04	13.9	*Chandra* HETG
10873	2009-03-01	18.1	*Chandra* HETG
0701981001	2013-02-03	47.8/49.0/36.4	*XMM-Newton* MOS1/MOS2/*pn*
0656580601	2014-03-01	31.4/31.2/17.1	*XMM-Newton* MOS1/MOS2/*pn*
0792382701	2016-08-23	19.8/19.6/17.0	*XMM-Newton* MOS1/MOS2/*pn*
0780950201	2018-02-07	41.9/41.3/35.7	*XMM-Newton* MOS1/MOS2/*pn*

2000,2001,2004 observations

From 12/2008 to 03/2009

- Hydrodynamical simulations were fit to the 2000-2010 data, demostrating that: SN1996cr exploded in a low-density medium before interacting with a dense shell of material at a distance <0.03pc from the explosion.
- The dense shell arose from the interaction of a WR wind with a previously RSG wind.

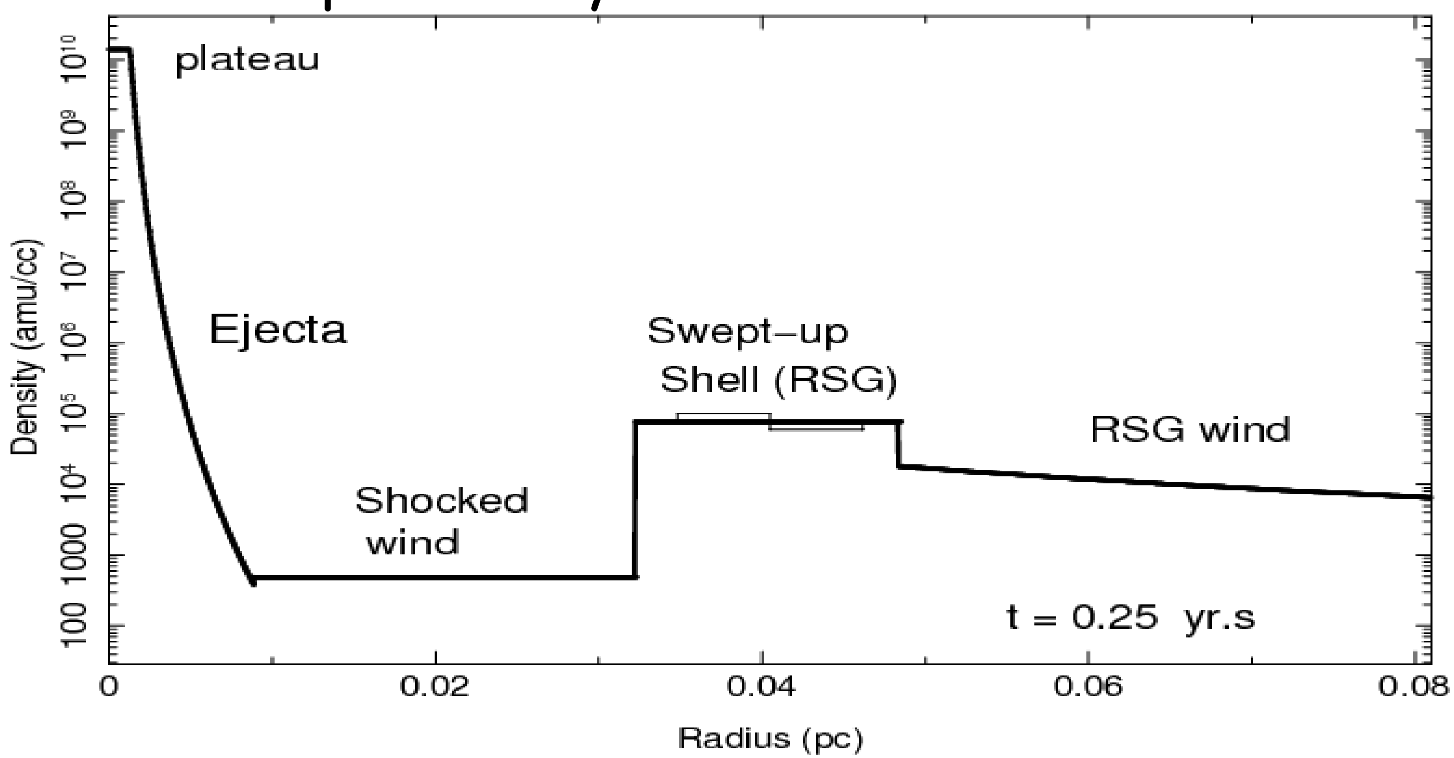

Dwarkadas +, 2010.

➢ Hydrodynamical model match well the light curve until 2009 epoch, as well as the spectra at 4 different epochs.

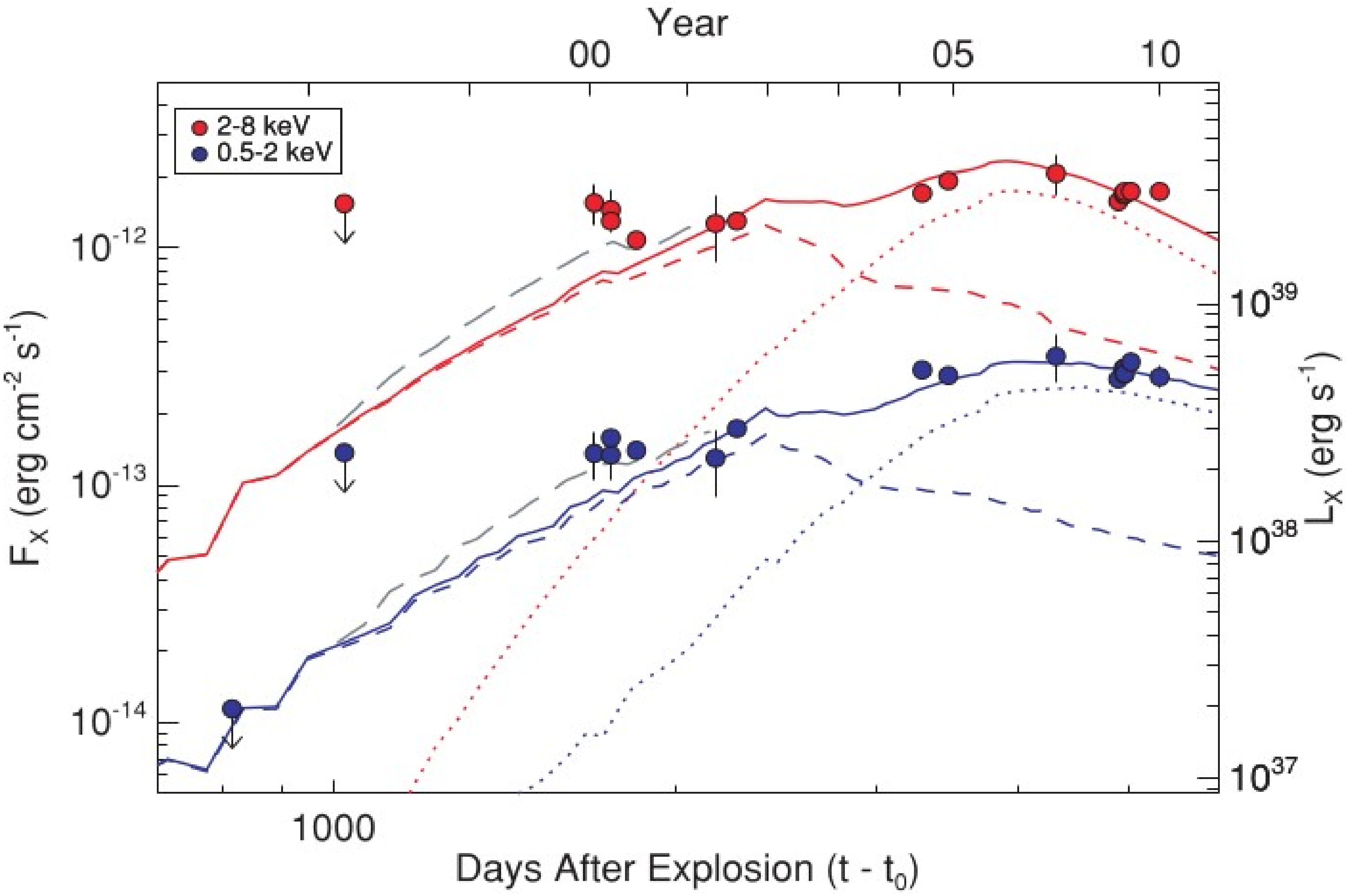

Dwarkadas +, 2010.

- Hydrodynamical model match well the light curve until 2009 epoch, as well as the spectra at 4 different epochs.

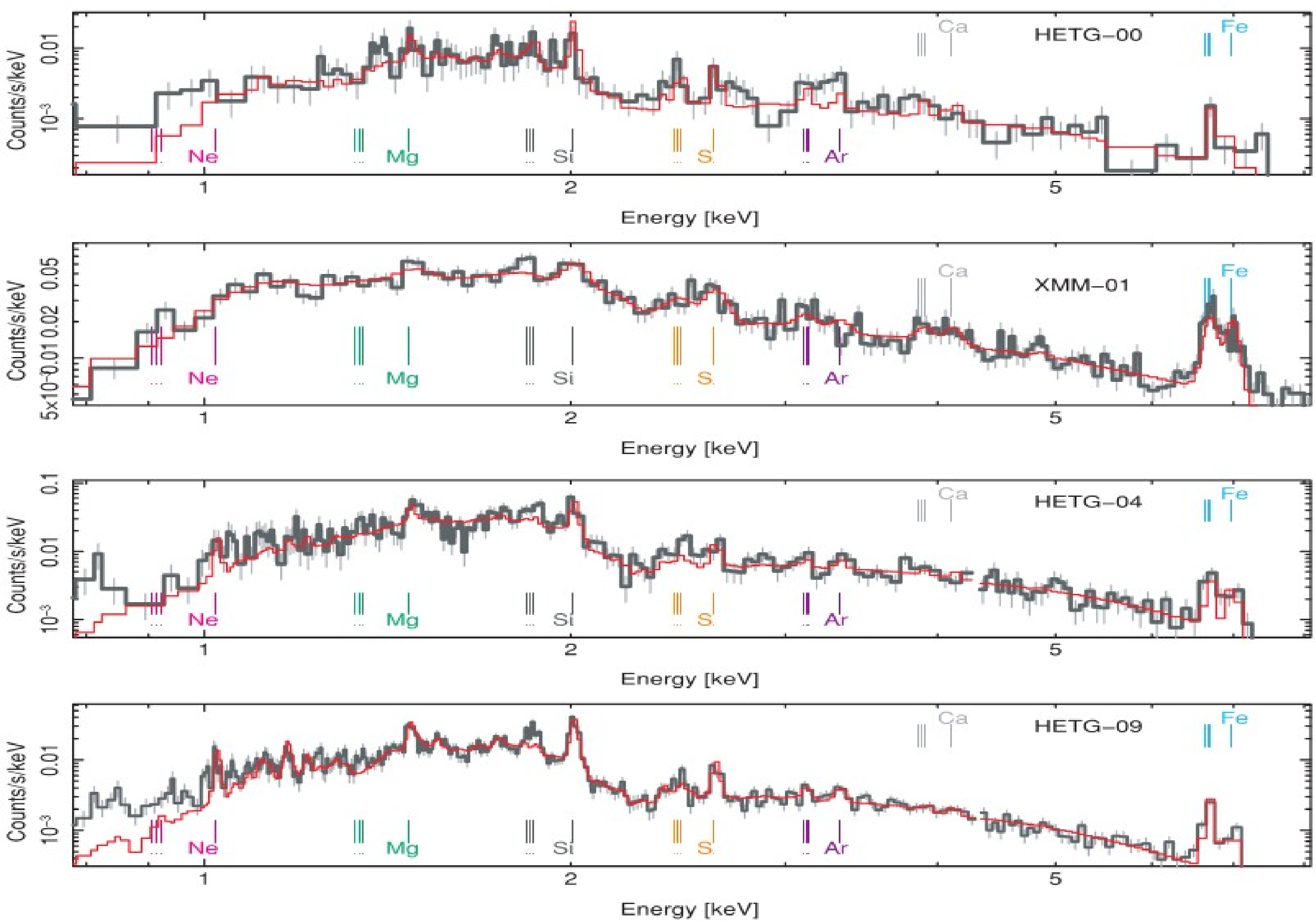

Dwarkadas +, 2010.

➢ However, 2009 campaign of SN1996cr also permits us analyze individual lines in X-ray bands. The line-shape give us information about the geometry of the ejecta-CSM interaction.

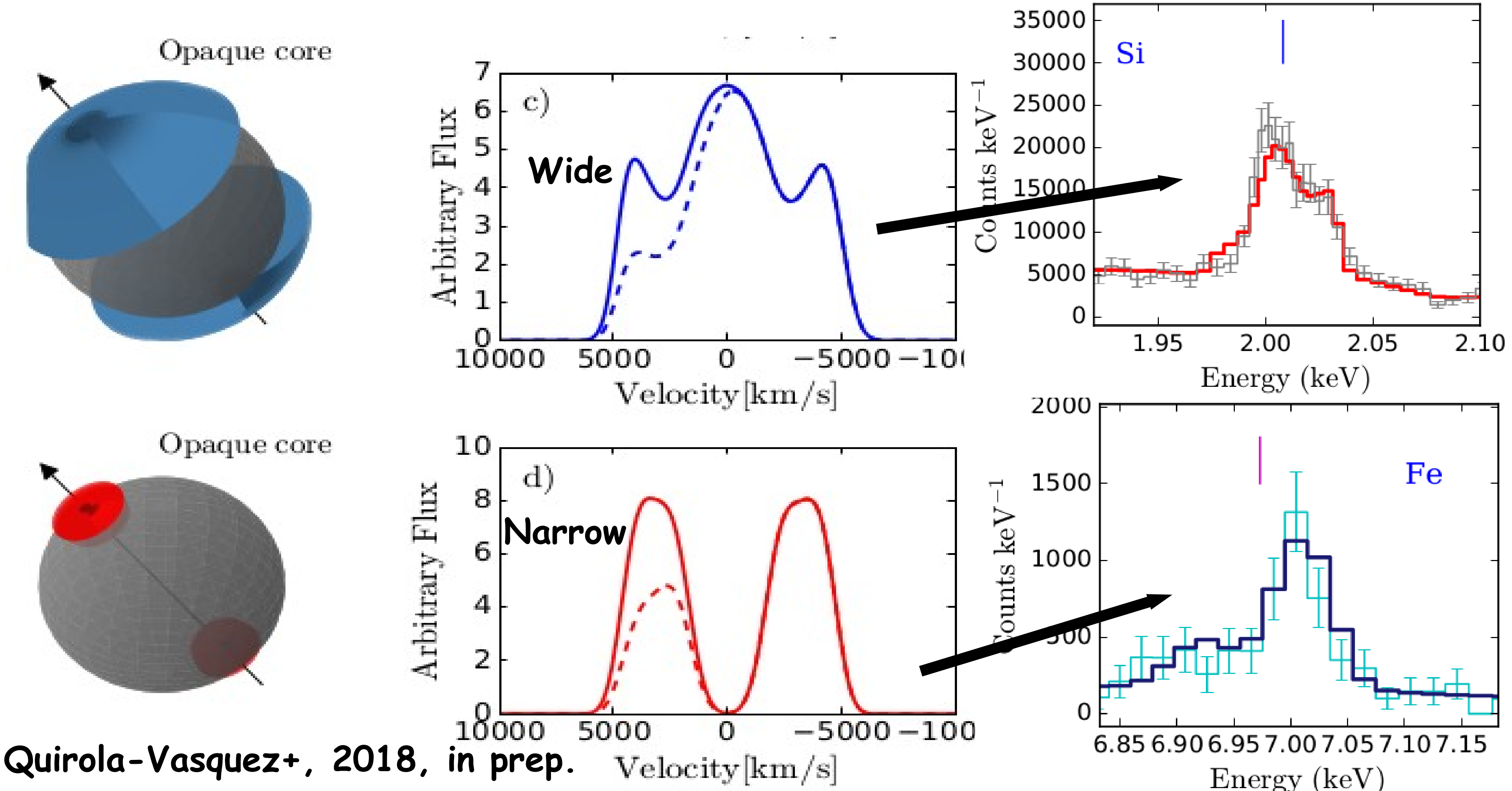

Quirola-Vasquez+, 2018, in prep.

- However, 2009 campaign of SN1996cr also permits us analyze individual lines in X-ray bands. The line-shape give us information about the geometry of the ejecta-CSM interaction.
- Two distinct polar shocks are required by the velocity profiles.

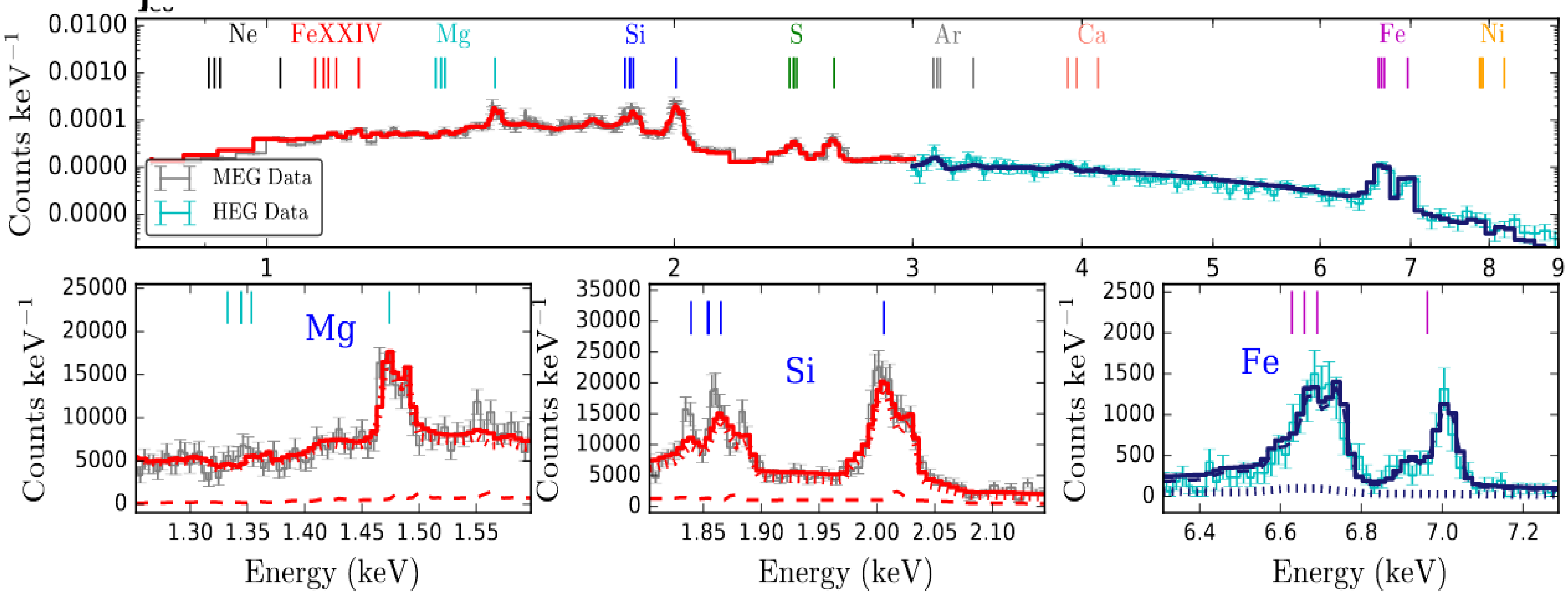

Quirola-Vasquez+, 2018, in prep.

- We applied this model to two decades of X-ray observations

ObsID	Date (UT)	Exposure (ks)	Instruments
374	2000-06-15	7.1	*Chandra* HETG
62877	2000-06-16	60.2	*Chandra* HETG
0111240101	2001-08-06	85.5/91.8/59.5	*XMM-Newton* MOS1/MOS2/*pn*
4770	2004-06-02	55.0	*Chandra* HETG
4771	2004-11-28	59.5	*Chandra* HETG
10223	2008-12-15	102.9	*Chandra* HETG
10224	2008-12-23	77.1	*Chandra* HETG
10225	2008-12-26	67.9	*Chandra* HETG
10226	2008-12-08	19.7	*Chandra* HETG
10832	2008-12-18	20.6	*Chandra* HETG
10833	2008-12-22	28.4	*Chandra* HETG
10842	2008-12-27	36.7	*Chandra* HETG
10843	2008-12-29	57.0	*Chandra* HETG
10844	2008-12-24	27.2	*Chandra* HETG
10850	2009-03-03	16.5	*Chandra* HETG
10872	2009-03-04	13.9	*Chandra* HETG
10873	2009-03-01	18.1	*Chandra* HETG
0701981001	2013-02-03	47.8/49.0/36.4	*XMM-Newton* MOS1/MOS2/*pn*
0656580601	2014-03-01	31.4/31.2/17.1	*XMM-Newton* MOS1/MOS2/*pn*
0792382701	2016-08-23	19.8/19.6/17.0	*XMM-Newton* MOS1/MOS2/*pn*
0780950201	2018-02-07	41.9/41.3/35.7	*XMM-Newton* MOS1/MOS2/*pn*

Quirola-Vasquez+, 2018, in prep.

- There may be SN1996cr-like objects still hidden in X-ray archives. Probably these SNe are located further away and thus weak enough that they remain unclassified.

- Importantly, the Fe and Si line EWs in X-ray SNe like SN1996cr should be a noticeable feature in the spectra of archive sources.

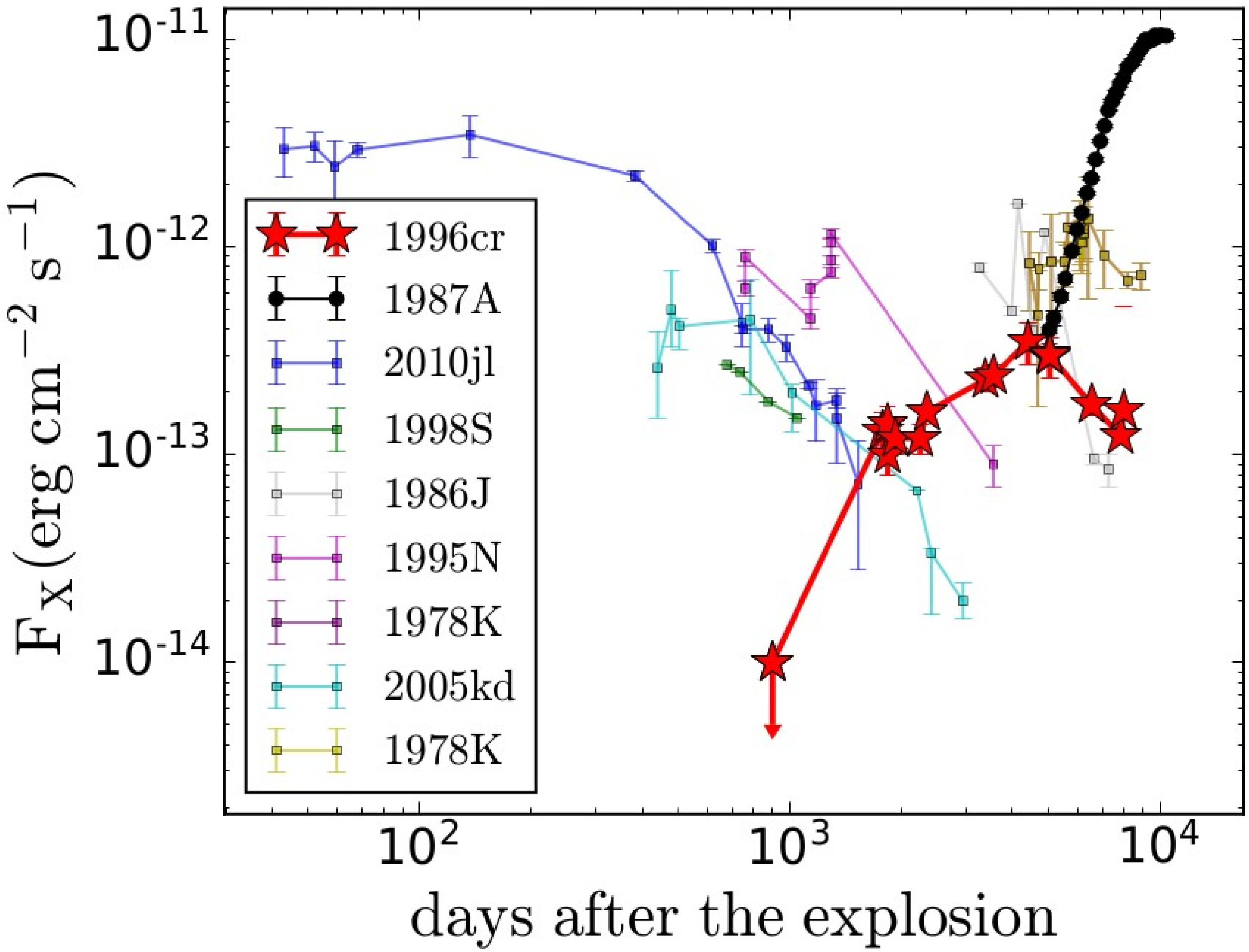

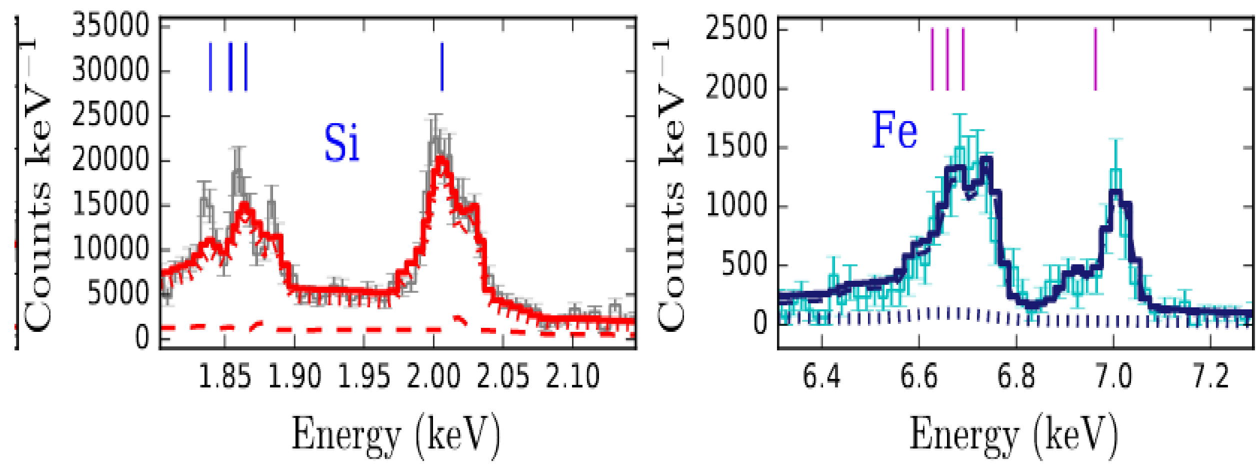

Quirola-Vasquez+, 2018, in prep.

- Future project: We are planing to use machine learning techniques to search for emission line objects in the Chandra and XMM archives.

Conclusions

- SN1996cr is an excellent case of study of a serendipitous archival discovery.
- With the amassed data we have been able to show that its progenitor star blew a CSM buble, and that the current ejecta-CSM shock is asymmetric, with both wide and narrow polar components.
- The number of SNe type IIn that emit in X-ray are low because a lot of factors. However, inside X-ray catalogs could exist more, waiting to be discovered.

X-ray transients

- I will start a project to use machine learning techniques to search for and chracterize X-ray transients in the Chandra and XMM archives.

A New, Faint Population of X-ray Transients

Franz E. Bauer,[1,2,3,4]★ Ezequiel Treister,[1,4,5] Kevin Schawinski,[6] Steve Schulze,[2,1]
Bin Luo,[7,8] David M. Alexander,[9] William N. Brandt,[10,11,12] Andrea Comastri,[13]
Francisco Forster,[14,2] Roberto Gilli,[13] David Alexander Kann,[15] Keiichi Maeda,[16,17]
Ken'ichi Nomoto,[17,18] Maurizio Paolillo,[19,20,21] Piero Ranalli,[22]
Donald P. Schneider,[10,11] Ohad Shemmer,[23] Masaomi Tanaka,[24] Alexey Tolstov,[17]
Nozomu Tominaga,[25] Paolo Tozzi,[26] Cristian Vignali,[27,13] Junxian Wang,[28]
Yongquan Xue[28] and Guang Yang[10,11]

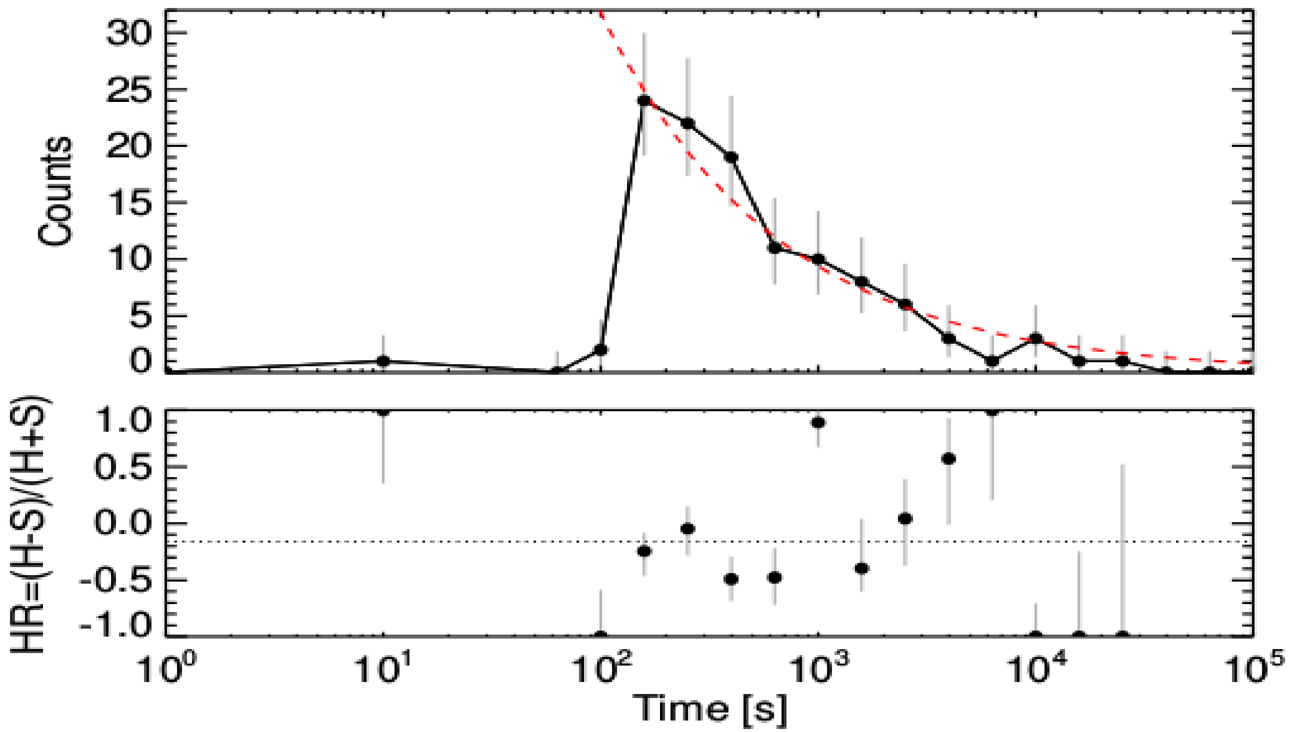

Figure 1. X-ray light curve (top panel) and hardness ratio (bottom panel) of CDF-S XT1. To highlight the sharp rise at ≈110 s, the 0.3–7.0 keV counts are logarithmically binned and shown with 1σ errors (Gehrels 1986); for this reason, binning here differs somewhat from that provided in Table 1. The red dashed curve denotes the best-fitting powerlaw decay time slope of a=−1.53. The hardness ratio, HR, and 1σ errors are calculated as $(H-S)/(H+S)$ following the Bayesian method of (Park et al. 2006), where S and H correspond to the 0.3–2.0 keV and 2.0–7.0 keV counts, respectively. We omit bins with no counts in the bottom panel, since HR values are completely unconstrained. The dotted horizontal line signifies the HR value expected for a Γ=1.43 power law.

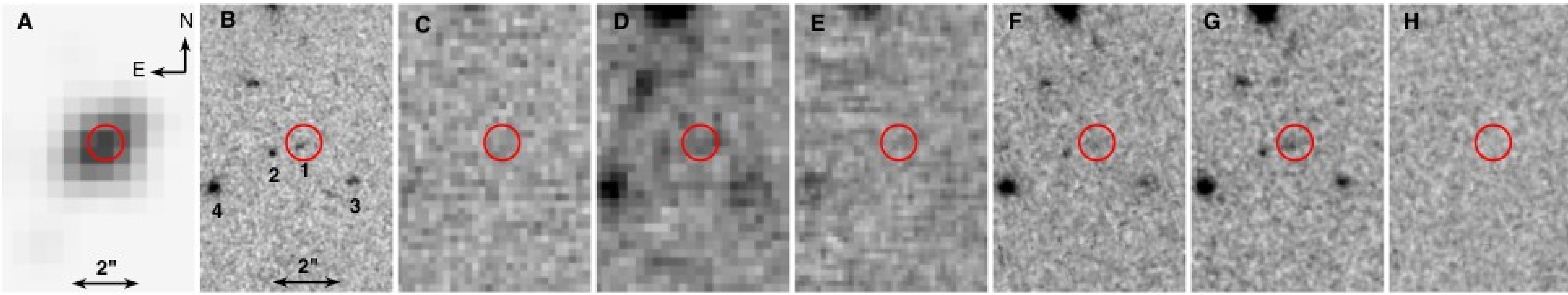

Figure 3. Images (6″×11″) in the vicinity of CDF-S XT1. From left to right: **(A)** *Chandra* ACIS-I 0.3–7.0 keV image of the transient detection acquired on 2014 October 01; **(B)** *HST*/ACS *F*606*W* image from GOODS-S acquired prior to 2008 (Giavalisco et al. 2004); **(C)** VLT/VIMOS *R*-band image serendipitously acquired on 2014 October 01 (80 min post-transient); **(D)** VLT/FORS2 *R*-band image acquired on 2014 October 18 (18 days post-transient); **(E)** Gemini/GMOS-S *r*-band image acquired on 2014 October 29 (27 days post-transient) **(F)** *HST*/WFC3 *F*110*W* image acquired on 2015 January 20 (111 days post-transient). **(G)** *HST*/WFC3 *F*125*W* image from CANDELS acquired prior to 2011 (Grogin et al. 2011; Koekemoer et al. 2011). **(H)** *F*110*W* – *F*125*W* difference image. A 0.″52 radius red circle denotes the 2σ X-ray positional error, centred on the X-ray transient position. The closest potential optical counterpart, seen clearly in the *HST* images and labeled #1 in (B), lies 0.″13 southeast of the X-ray position and has a magnitude of $m_{\rm R}$=27.5 mag. It is classified as a dwarf galaxy with $z_{\rm ph}$=2.23. This galaxy appears marginally detected in the 1 hr FORS2 image, but not in the VIMOS or GMOS-S images. Three other sources are labeled and discussed in the text. No transient is observed in the *HST* difference image (final panel).

- Presumably, there should be more fast transients like CDF-S X-1 in the archives. One of the goals of my project is to find more and/or place firm limits on their rate.
- I look forward to talking with you about both SNe and fast X-ray transients during this meeting.

Astronomy's next big discovery may be hiding in piles of old data.

THANKS

Additional slides

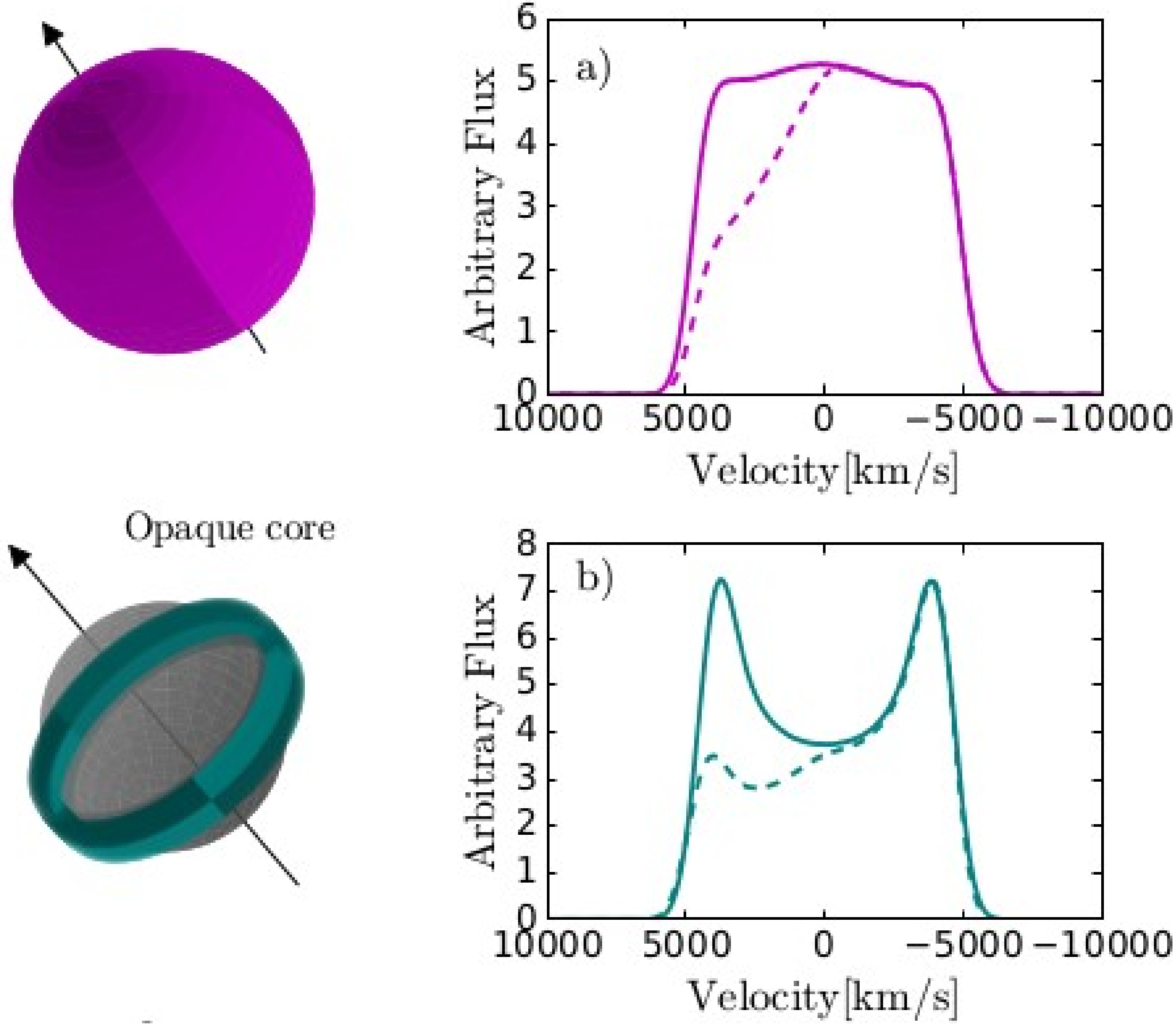

Opaque core
a)
b)
Arbitrary Flux
Velocity[km/s]
10000
5000
0
−5000
−10000
0
1
2
3
4
5
6
7
8

- **El mejor modelo fue:**

TBabs(shellblur*vpshock)+TBabs(shellblur*vpshock)

alta temp., emisión polar | **baja temp., emisión polar**

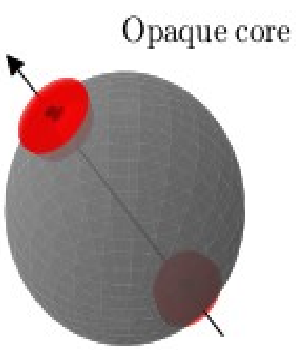

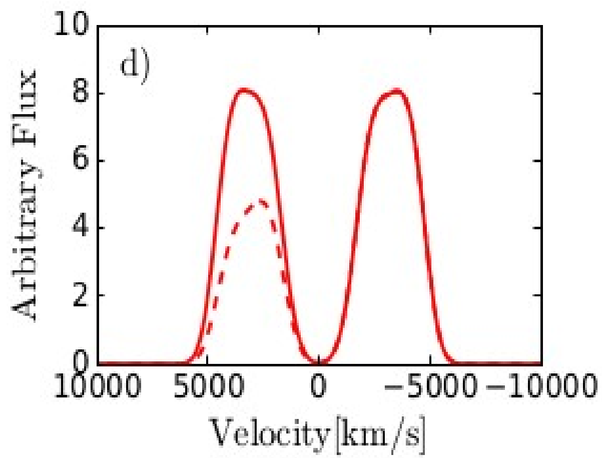

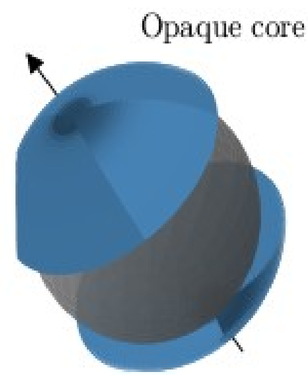

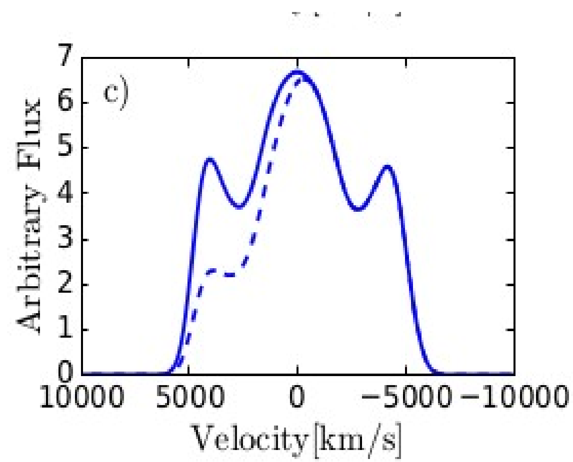

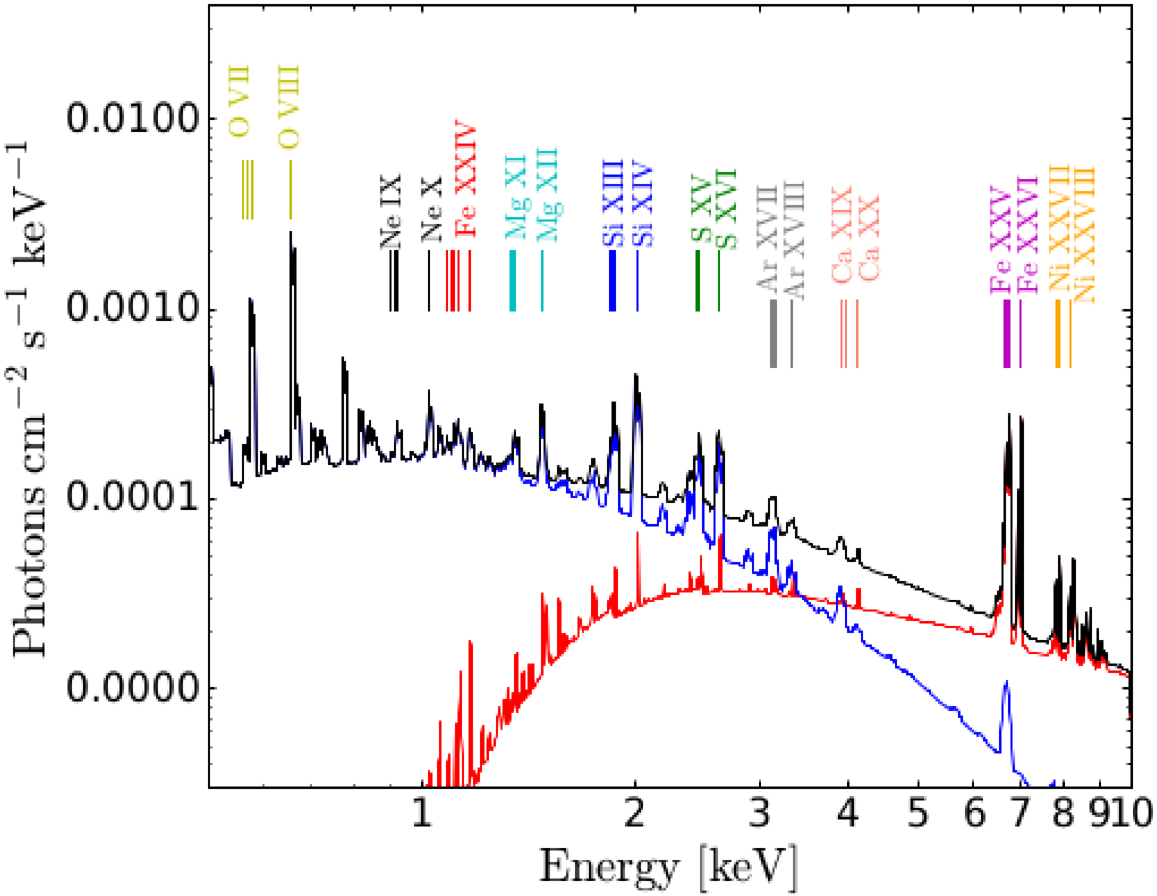

Figure 7. Best-fit model M5 spectrum (*black* line) between 0.3–10 keV in units of Photons cm^{-2} s^{-1} keV^{-1}. The higher and lower temperature components are denoted in *red* and *blue*, respectively. The color vertical lines mark the most intense lines of the H-like and He-like ions of high-Z elements.